Hierarchies of geometric entanglement

M. Blasone,[1,2] F. Dell'Anno,[1,2,3,4] S. De Siena,[1,2,3,4] and F. Illuminati[1,2,3,4,5,*]
[1]*Dipartimento di Matematica e Informatica, Università degli Studi di Salerno, Via Ponte don Melillo, I-84084 Fisciano (SA), Italy*
[2]*Gruppo Collegato di Salerno, INFN Sezione di Napoli, Salerno, Italy*
[3]*CNR-INFM Coherentia, Napoli, Italy*
[4]*CNISM Unità di Salerno, Salerno, Italy*
[5]*ISI Foundation for Scientific Interchange, Viale Settimio Severo 65, 00173 Torino, Italy*
(Received 25 December 2007; published 3 June 2008)

We introduce a class of generalized geometric measures of entanglement. For pure quantum states of N elementary subsystems, they are defined as the distances from the sets of K-separable states ($K=2,\ldots,N$). The entire set of generalized geometric measures provides a quantification and hierarchical ordering of the different bipartite and multipartite components of the global geometric entanglement, and allows discrimination among the different contributions. The extended measures are applied to the study of entanglement in different classes of N-qubit pure states. These classes include W and Greenberger-Horne-Zeilinger (GHZ) states, and their symmetric superpositions; symmetric multimagnon states; cluster states; and, finally, asymmetric generalized W-like superposition states. We discuss in detail a general method for the explicit evaluation of the multipartite components of geometric entanglement, and we show that the entire set of geometric measures establishes an ordering among the different types of bipartite and multipartite entanglement. In particular, it determines a consistent hierarchy between GHZ and W states, clarifying the original result of Wei and Goldbart that W states possess a larger global entanglement than GHZ states. Furthermore, we show that all multipartite components of geometric entanglement in symmetric states obey a property of self-similarity and scale invariance with the total number of qubits and the number of qubits per party.

DOI: 10.1103/PhysRevA.77.062304 PACS number(s): 03.67.Mn, 03.65.Ud

I. INTRODUCTION

Quantification of pure state bipartite entanglement, a concept that emerged immediately after the first systematization of quantum mechanics [1], is by now well understood in terms of the entropic content in the reduced states of the constituent subsystems, as lucidly pointed out for the first time by Schrödinger [2]. The universal properties that any *bona fide* measure of entanglement has to satisfy have been thoroughly discussed and characterized in recent years [3–6]. For pure states of bipartite systems, the von Neumann entropy is the unique measure of entanglement, and all other consistent measures are monotonic functions of the former [7]. However, this uniqueness is lost in bipartite mixed states: In this context, measures that differ according to their definitions and/or operational meaning, such as, for instance, the entanglement of formation, the distillable entanglement, the relative entropy of entanglement, and the negativity [4,8,9], quantify different forms of entanglement. In fact, very few of these quantities can be computed explicitly for mixed quantum states, even in the simplest instances. A notable exception is the celebrated Wootters formula for the entanglement of formation of arbitrary two-qubit mixed states, obtained in terms of the concurrence [10,11].

The situation becomes even more complex in the multipartite instance, already at the level of pure states in finite-dimensional Hilbert spaces. Progress has been achieved mainly in understanding the different ways in which multipartite systems can be entangled. The intrinsic nonlocal character of entanglement imposes invariance and monotonicity constraints under local quantum operations. Equivalence classes of entangled states can be defined with respect to the group of reversible stochastic local quantum operations assisted by classical communication (SLOCC) [12]. Such an approach has allowed the demonstration that three and four qubits can be entangled, respectively, in two and nine different inequivalent ways [13,14]. In the case of three qubits, the representatives of the two inequivalent classes are, notoriously, the W and Greenberger-Horne-Zeilinger (GHZ) states [13,15].

Simplifying to the essentials, in a multipartite scenario a legitimate quantification of entanglement can be achieved by identifying a positive function that is an entanglement monotone (vanishing on separable states and not increasing under SLOCC), and is endowed with some kind of operational interpretation. Several measures satisfying these requirements have been proposed. For a system of three qubits, Wootters and co-workers defined the so-called residual entanglement, or three-tangle, a quantity constructed as the difference between the squared three-qubit concurrence and the squared concurrences of the reduced two-qubit states [16]. While successfully detecting the genuine tripartite entanglement in the state $|\mathrm{GHZ}^{(3)}\rangle$, the three-tangle (or residual tangle) vanishes if computed for the state $|W^{(3)}\rangle$, thus being inappropriate for the quantification of tripartite entanglement in this class of states. In other words, a nonvanishing residual tangle is a sufficient but not necessary condition for the detection of genuine multipartite entanglement. The Schmidt measure, defined as the minimum of $\log_2 r$ with r being the minimum of the number of terms in an expansion of a quantum state in product basis, has been proposed by Eisert and Briegel as an alternative measure of multipartite entanglement [17]. Other

*Corresponding author. illuminati@sa.infn.it

proposals are given as functions of the various bipartite entanglements contained in a multipartite state [18–22]. The seed representative of this class of measures is the global entanglement of Meyer and Wallach, that for an N-qubit state is defined as the sum of all the possible two-qubit concurrences [18].

A different set of entanglement quantifiers is defined in purely geometric terms. The relative entropy of entanglement (generalized for multipartite settings) and the so-called geometric entanglement belong to this class [23–25]. The relative entropy of entanglement is defined as the distance of a given state from the set of fully separated states, quantified in terms of the quantum relative entropy [23]. The geometric entanglement was originally defined as the Euclidean distance of a given multipartite state to the nearest fully separable state [24–26]. This last measure can be considered as one of the most reliable quantifiers of global multiparticle entanglement [27]: It exhibits interesting connections with other measures [26,28] and can be efficiently estimated by quantitative entanglement witnesses amenable of experimental verification [29,30]. Given an N-partite pure state $|\Psi\rangle$, the geometric measure of entanglement introduced by Wei and Goldbart [26] is defined as

$$E_G(|\Psi\rangle) = 1 - \max_{|\Phi\rangle} |\langle \Phi|\Psi\rangle|^2, \tag{1}$$

where the maximum is taken with respect to all pure states that are fully factorized, i.e., the N-separable states

$$|\Phi\rangle = \bigotimes_{s=1}^{N} |\Phi_s\rangle, \tag{2}$$

where the states $|\Phi_s\rangle$ are single-qubit pure states. This measure is intrinsically geometric because it coincides with the distance (in the Hilbert-Schmidt norm) between a given pure state and the set of fully separable (i.e., fully product) pure states. The Wei-Goldbart geometric measure is thus a global quantifier of entanglement, including all the bipartite and multipartite contributions.

The geometric measure can be extended by the convex roof procedure to the case of mixed states, and, analogously to the Meyer-Wallach global entanglement, is a proper multipartite entanglement monotone. Remarkably, the geometric measure can be effectively exploited to quantify the entanglement of two distinct multipartite bound entangled states [31] and to study the behavior of global entanglement at the approach of quantum phase transitions [32–34]. However, notwithstanding the very appealing properties and the important results cited above, the global nature of the Wei-Goldbart geometric entanglement constitutes a limitation insofar as it does not allow one to distinguish and discriminate among the different bipartite and multipartite contributions to the overall entanglement, to determine their properties, and to establish a systematic hierarchy among them. It is the aim of the present work to fill this gap.

In this paper, we define and study in detail a natural and powerful multipartite generalization of the geometric measure of entanglement for pure states of many-qubit systems. We first introduce a compact and convenient parametrization to express analytically general K-separable states of N-qubit systems ($K \leq N$). We then analyze the behavior of the distance between pure N-qubit states and the set of K-separable states ($K=2,\ldots,N$) in order to determine and distinguish the different multipartite contributions to the geometric entanglement and characterize their ordering. The different distances, corresponding to $K=2,\ldots,N$, quantify hierarchically the different forms of multipartite entanglement present in the given N-qubit state. In Sec. II, we define the multicomponent generalization of the geometric measure, we review the known results in the case of full separability and, for this latter case, we also present some further extended results. In Sec. III we evaluate explicitly the generalized multicomponent geometric measure of entanglement, considering genuine K separability ($K \leq N$). We analyze the detailed behavior of the different forms of geometric entanglement for various relevant classes of N-qubit states, establishing some generic and asymptotic properties, and we determine the explicit hierarchy holding for W, GHZ, cluster, and multimagnon states. In the case of W and GHZ states, the established relations between the different forms of multipartite geometric entanglement clarify the original result of Wei and Goldbart that W states possess a larger total entanglement content than GHZ states, when quantified by the geometric measure. Moreover, in the case of N-qubit W states, we find that the geometric entanglement is scale invariant (self-similar) as the total number of qubits grows at the same rate as the number of subsystems in each party. We show that the property of self-similarity is enjoyed by other symmetric states as well, as a direct consequence of the invariance under permutation of any two qubits, which is the characterizing property of symmetric states. We then analyze and determine the different multipartite components of geometric entanglement for arbitrary symmetric superpositions of N-qubit GHZ and W states. In Sec. IV we compute the multipartite geometric measures for classes of generalized W states beyond the single-excitation regime; these are general symmetric states, the so-called magnon states, that are of crucial importance, for instance, in the theory of magnetism. Furthermore, we determine the multipartite components of geometric entanglement in generalized, asymmetric W-like superposition states. In this and related cases, at variance with most of the symmetric instances, a complete characterization of entanglement requires the determination of all the multipartite geometric components, which we compute explicitly. Finally, in Sec. V we discuss some general conjectures on generic properties and typical behaviors of the geometric entanglement, and examine some outlooks on possible future lines of research.

II. GEOMETRIC ENTANGLEMENT: *K* SEPARABILITY VS FULL SEPARABILITY

Let us consider an N-qubit system, corresponding to a tensor-product state space $\mathcal{H}^{d_N}$ of dimension $d_N=2^N$. For such a system, let us introduce the integer K, $2 \leq K \leq N$, and the ordered sequence of integers $\{M_1, M_2, \ldots, M_K\}$, where $M_1 \leq M_2 \leq \cdots \leq M_K$, and $\Sigma_{s=1}^{K} M_S = N$. Let us consider the K partition of the system in K subsystems described by the sets $\{Q_s\}_{s=1}^{K}$. Let each set Q_s be composed of M_s elementary par-

ties, i.e., $Q_s=\{i_1^{(s)},i_2^{(s)},\ldots,i_{M_s}^{(s)}\}$, where $i_j^{(s)}\in\{1,\ldots,N\}$ is a discrete index labeling the N elementary parties, and $Q_s\cap Q_{s'}=\emptyset$ for $s\neq s'$. Given a generic K partition $Q_1|\,Q_2|\cdots|Q_K$ of the N-qubit system, any K-separable state associated with such a partition is defined as the tensor product of K M_s-qubit pure states $|\Phi_s^{(Q_s)}\rangle$. Each state $|\Phi^{(Q_s)}\rangle$ belongs to the Hilbert space $\mathcal{H}^{d_{Q_s}}$ of dimension $d_{Q_s}=2^{M_s}$. A K-separable state can then be written as

$$\bigotimes_{s=1}^{K}|\Phi_s^{(Q_s)}\rangle. \tag{3}$$

Correspondingly, the Hilbert space $\mathcal{H}^{d_N}$ is decomposed into the tensor product $\otimes_{s=1}^{K}\mathcal{H}^{d_{Q_s}}$. Varying the integers M_s, one obtains different K partitions $Q_1|\,Q_2|\cdots|Q_K$ and, correspondingly, different possible K-separable states. It is worth noticing that even at fixed $M_1|\,M_2|\cdots|M_K$, there exist different K partitions associated with the different arrangements of the elementary parties in the sets Q_s; in fact, from a given initial K partition, a certain number of different K partitions can be generated through permutations of the elementary parties belonging to different sets Q_s. We then denote by $\mathbf{S}_K$ the set of all K-separable states, defined as

$$\mathbf{S}_K=\bigcup_{\{Q_1,\ldots,Q_K\}}S_K(Q_1|\cdots|Q_K), \tag{4}$$

where $S_K(Q_1|\,Q_2|\ldots|Q_K)$ is the set of all the K-separable states associated with a fixed K partition. We can now define the relative (i.e., partition-dependent) and the absolute (i.e., partition-independent) geometric measures of entanglement with respect to K-separable pure states for an arbitrary N-qubit pure state $|\Psi^{(N)}\rangle$, respectively, as

$$E_G^{(K)}(Q_1|\cdots|Q_K)=1-\Lambda_K^2(Q_1|\cdots|Q_K), \tag{5}$$

where the squared overlap

$$\Lambda_K^2(Q_1|\cdots|Q_K)=\max_{|\varphi\rangle\in S_K(Q_1|\cdots|Q_K)}|\langle\varphi|\Psi^{(N)}\rangle|^2, \tag{6}$$

and

$$E_G^{(K)}(|\Psi^{(N)}\rangle)=1-\Lambda_K^2(|\Psi^{(N)}\rangle), \tag{7}$$

where the squared overlap

$$\Lambda_K^2(|\Psi^{(N)}\rangle)=\max_{|\Phi\rangle\in\mathbf{S}_K}|\langle\Phi|\Psi^{(N)}\rangle|^2. \tag{8}$$

By Eqs. (5), (6), and (8), the quantity (7) measures the absolute minimum distance of a state from the set of all K-separable states. Equivalently, $E_G^{(K)}(|\Psi^{(N)}\rangle)=\min_{\{S_K(Q_1|\cdots|Q_K)\}}E_G^{(K)}(Q_1|\cdots|Q_K)$. Trivially, for any N partition (i.e., $K=N$), one has $M_1=M_2=\cdots=M_N=1$ and N separability coincides with full separability, while 1 separability is a common feature of any state, i.e., $E_G^{(1)}=0$ for all states $\{|\Psi^{(N)}\rangle\}$. In the particular instance of symmetric states, which are states invariant under the permutation of any two qubits, the quantities $E_G^{(K)}(Q_1|\cdots|Q_K)$ and $\Lambda_K^2(Q_1|\cdots|Q_K)$ satisfy the same invariance property. Therefore, in such a case, in the definitions (5) and (6), the symbols Q_s can be replaced by the indices M_s as the multi-index $M_1|\cdots|M_K$ completely determines the particular component of geometric entanglement. In Ref. [26], the measure (7) is defined only in the simplest instance of N separability. In this case, we may write the general expression for a (normalized) K-separable state $|\Phi\rangle$, Eq. (2), in the following Hartree form:

$$|\Phi\rangle=\bigotimes_{l=1}^{N}(\cos\Gamma_l|0\rangle_l+e^{i\Delta_l}\sin\Gamma_l|1\rangle_l), \tag{9}$$

with Γ_l and Δ_l real. By using Eq. (9) with $\Delta_l=0$, the geometric measure of entanglement can be analytically computed for the classes of GHZ and W states. The definition of these states for the N-qubit case reads

$$|\mathrm{GHZ}^{(N)}\rangle=\frac{1}{\sqrt{2}}\sum_{i=1}^{2}|\delta_{i,2}\delta_{i,2}\cdots\delta_{i,2}\rangle, \tag{10}$$

$$|W^{(N)}\rangle=\frac{1}{\sqrt{N}}\sum_{i=1}^{N}|\delta_{i,1}\delta_{i,2}\cdots\delta_{i,N}\rangle, \tag{11}$$

where $\delta_{i,j}$ denotes the Kronecker delta, and $|e^{(1)}e^{(2)}\cdots e^{(N)}\rangle\equiv|e^{(1)}\rangle_1|e^{(2)}\rangle_2\cdots|e^{(N)}\rangle_N$ $(e^{(j)}=0,1)$. The GHZ and W states are fully symmetric, i.e., invariant under the exchange of any two qubits, and greatly differ from each other in their correlation properties. On general grounds [17], one can expect that N-qubit GHZ states must possess N-partite but no K-partite entanglement for $K<N$. On the other hand, the N-qubit W states do possess K-partite entanglement for $K<N$.

For the total geometric entanglement of states $|\mathrm{GHZ}^{(N)}\rangle$ and $|W^{(N)}\rangle$, measured with respect to the set of N-separable (i.e., fully separable) states, the following relations hold [26]:

$$\Lambda_N^2(|\mathrm{GHZ}^{(N)}\rangle)=\frac{1}{2}, \tag{12}$$

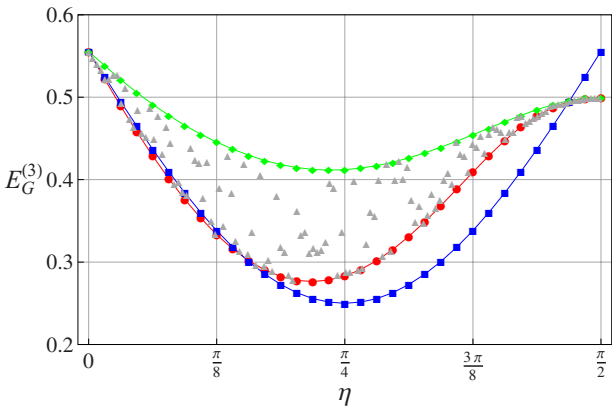

FIG. 1. (Color online) $E_G^{(3)}$ for the superposition of $|W^{(3)}\rangle$ and $|\tilde{W}^{(3)}\rangle$ states, Eq. (18), and for the superposition of $|W^{(3)}\rangle$ and $|\mathrm{GHZ}^{(3)}\rangle$ states, Eq. (19), as a function of the mixing angle η. $E_G^{(3)}$ for the state (19) is plotted for the following choices of the free relative phase ϕ: $\phi=0$ (round points, in red), π (diamond points, in green), and taking random values in the range $[0,\pi]$ (triangle points, in gray). $E_G^{(3)}$ for the state (18) does not depend on ϕ (box points, in blue). All plotted quantities are dimensionless.

$$\Lambda_N^2(|W^{(N)}\rangle) = \left(\frac{N-1}{N}\right)^{N-1}. \tag{13}$$

In particular, Eq. (13) is obtained by setting $\Gamma_l = \arcsin(1/\sqrt{N})$, with $l=1,\ldots,N$. Therefore, for the $|\mathrm{GHZ}^{(N)}\rangle$ states, the total geometric entanglement takes the constant value 1/2, independently of N. On the other hand, for the $|W^{(N)}\rangle$ states, the total geometric entanglement grows with N, converging to a simple function of the Neper number in the asymptotic limit:

$$E_G^{(3)}(|W^{(3)}\rangle) = \frac{5}{9} \approx 0.555, \tag{14}$$

$$E_G^{(4)}(|W^{(4)}\rangle) = \frac{37}{64} \approx 0.578, \tag{15}$$

$$\vdots$$

$$E_G^{(N)}(|W^{(N)}\rangle) = 1 - \left(\frac{N-1}{N}\right)^{N-1}, \tag{16}$$

$$\vdots$$

$$\lim_{N\to\infty} E_G^{(N)}(|W^{(N)}\rangle) = 1 - e^{-1} \approx 0.632. \tag{17}$$

Therefore, according to the measure of total geometric entanglement, the W states are overall more entangled than GHZ states for any N, notwithstanding the fact that the latter must always possess a larger amount of genuine N-partite entanglement. Moreover, the asymptotic limit acquired by the total geometric entanglement on W states for large N appears to point at some underlying topological structure.

In the first nontrivial multipartite case $N=3$, interesting results have been obtained also for superposition states of the form [26]

$$|W\ \tilde{W}^{(3)}\rangle = \cos\ \eta|W^{(3)}\rangle + e^{i\phi}\ \sin\ \eta|\tilde{W}^{(3)}\rangle, \tag{18}$$

$$|W\ \mathrm{GHZ}^{(3)}\rangle = \cos\ \eta|W^{(3)}\rangle + e^{i\phi}\ \sin\ \eta|\mathrm{GHZ}^{(3)}\rangle, \tag{19}$$

where the mixing angle η lies in the range $[0,\frac{\pi}{2}]$, ϕ is a free relative phase, and $|\tilde{W}^{(3)}\rangle = \frac{1}{\sqrt{3}}(|110\rangle + |101\rangle + |011\rangle)$. The geometric entanglement is computed with respect to the fully three-separable state [Eq. (9) with $N=3$]. In Fig. 1, $E_G^{(3)}$ for the states (18) and (19) is plotted as a function of η.

The geometric measure of entanglement for the state (18) attains its maximum 5/9 at $\eta=0,\pi/2$ and its minimum at $\eta=\pi/4$, and is independent of the phase ϕ; on the contrary, for the state (19) it exhibits an explicit dependence on ϕ that is maximized for $\phi=\pi$ and attains its maximum value 5/9 at $\eta=0$. The free relative phase ϕ cannot be eliminated by local unitary operations (in the sense of being of dimension less than N) for states of the form (19), but only by means of global N-dimensional transformations. Therefore, the global entanglement content of these states must necessarily depend on ϕ, and the latter thus acquires the meaning of a global geometric phase.

III. MULTIPARTITE COMPONENTS OF GEOMETRIC ENTANGLEMENT

As discussed above, the distance of an N-partite state $|\Psi^{(N)}\rangle$ from the set of fully separable (i.e., N-separable) states is a legitimate quantifier of a global form of entanglement, encompassing N-partite, $(N-1)$-partite, …, and bipartite components in an indistinguishable way. This observation motivates the search for a more refined geometric quantification of entanglement, in order to distinguish the different multipartite contributions. To this end, we proceed to study the distances of $|\Psi^{(N)}\rangle$ from the various sets of K-separable states, as defined in the previous section. For a fixed K ($K=2,\ldots,N$), the distance Eq. (7) quantifies the N-partite, …, $(N-K+2)$-partite contributions to the global entanglement. Moreover, it is evident that, for each K,

$$\mathbf{S}_{K-1} \supseteq \mathbf{S}_K, \quad E_G^{(K-1)}(|\Psi^{(N)}\rangle) \leq E_G^{(K)}(|\Psi^{(N)}\rangle), \tag{20}$$

where the second inequality follows by the law of set inclusion. Some simple examples may be of help to elucidate the structure of this hierarchy. Let us take $N=3$. In this case, we have two possibilities: $K=2,3$. For $K=2$ one has information only on the pure tripartite (three-qubit) component of the geometric entanglement, while for $K=3$ (distance from the fully separable states) one has indistinguishable information on both three- and two-qubit entanglement. Moreover, as already mentioned above, since the set of biseparable states $S_2(1|2)$ contains the set of three-separable states $S_3(1|1|1)$, it follows that $E_G^{(2)}(|\Psi^{(3)}\rangle) \leq E_G^{(3)}(|\Psi^{(3)}\rangle)$. If equality holds, it then follows that the entire content of entanglement is due only to the tripartite contribution. The extension to higher dimensions $N\geq 4$ is straightforward, although the number of possible partitions quickly grows. On the other hand, we will show that the genuine N-partite entanglement of GHZ and W states is always associated with the distance from the set of biseparable states $S_2(1|N-1)$.

We shall now introduce some concise notations that will be useful in the following. Let us denote by $|\chi^{(M)}\rangle$ an arbitrary M-partite qubit state, which can be expressed in the form

$$|\chi^{(M)}\rangle = \sum_{j_1,\ldots,j_M=0}^{1} c_{j_1,\ldots,j_M}|j_1\cdots j_M\rangle, \tag{21}$$

where $c_{j_1,\ldots,j_M}$ are complex parameters satisfying the normalization constraint $\Sigma_{j_1,\ldots,j_M=0}^{1}|c_{j_1,\ldots,j_M}|^2=1$. In order to simplify the notation, we substitute the multi-index $(j_1,\ldots,j_M)$ by the single index $J=\Sigma_{q=1}^{M}2^{M-q}j_q$ (i.e., summation in the binary system), so that Eq. (21) reads

$$|\chi^{(M)}\rangle = \sum_{J=0}^{d_M-1} c_J|J\rangle\rangle_M. \tag{22}$$

Obviously, one has $0\leq J\leq d_M-1=2^M-1$. This notation provides a useful ordering of the states based on the binary numbering. In fact, the index $J=0,1,2\ldots,2^M-1$ labels, respectively, the states $|00\ldots00\rangle, |00\ldots01\rangle, |00\ldots10\rangle, \ldots, |11\ldots11\rangle$. Let us note that the states $|J\rangle\rangle_M$ satisfy the orthonormality relation, i.e., ${}_M\langle\langle J|J'\rangle\rangle_M = \delta_{J,J'}$; moreover, each M-qubit state $|J\rangle\rangle_M$ can

be written in the decomposed form $|J\rangle\rangle_M = |J_1\rangle\rangle_{M_1} \otimes |J_2\rangle\rangle_{M_2}$, where $M=M_1+M_2$, and $J=2^{M_2}J_1+J_2$. Using the Euler representation and eliminating an irrelevant global phase factor, the parameters c_J can be cast in the form $c_J = r_J e^{i\phi_J}$, where $r_J=|c_J|$, $\phi_0=0$, and the phases ϕ_J are arbitrary for $J>1$. It is worth noting that the fully separable state (9) is a particular realization of $|\chi^{(M)}\rangle$ for $M=N$. The K-separable state given by Eq. (3), can be expressed explicitly by using, for each state $|\Phi_s^{(M_s)}\rangle$, the general form (22) and the hyperspherical parametrization introduced in Appendix A [see Eq. (A1)]. The hyperspherical parametrization will then prove extremely convenient in the computation of Eq. (8) for any value of the index K. By using the notation in terms of the binary-numbering index, Eqs. (10) and (11) can be recast as

$$|\mathrm{GHZ}^{(N)}\rangle = \frac{1}{\sqrt{2}}(|0\rangle\rangle_N + |2^N-1\rangle\rangle_N), \tag{23}$$

$$|W^{(N)}\rangle = \frac{1}{\sqrt{N}}\sum_{p=0}^{N-1} |2^p\rangle\rangle_N. \tag{24}$$

In the next sections we will determine the different multipartite contributions for some relevant classes of states symmetric under exchange of any pair of qubits.

A. Three-qubit pure states

We begin by considering three-qubit pure states, the simplest nontrivial instance of multipartite states. In this case, given the tensor product Hilbert space $\mathcal{H}^{(8)}=\mathcal{H}^{(2)}\otimes\mathcal{H}^{(2)}\otimes\mathcal{H}^{(2)}$, associated with a system of $N=3$ qubits, there are only two sets of separable states: the set $\mathbf{S}_2$ of biseparable states ($K=2$), and the set $\mathbf{S}_3$ of three-separable states ($K=3$, full separability), with $\mathbf{S}_2 \supseteq \mathbf{S}_3$. The distance $E_G^{(3)}$ from the set $\mathbf{S}_3$ measures the global geometric entanglement of Wei and Goldbart, while the distance $E_G^{(2)}$ from the set S_2 measures the genuine tripartite contribution to the global geometric entanglement $E_G^{(2)} \leq E_G^{(3)}$, with equality holding when all the entanglement is due only to the genuine tripartite component and there is no bipartite component. The general expression for any biseparable state $|\Phi\rangle$ is of the form

$$|\Phi\rangle = |\Phi_1^{(1)}\rangle_k \otimes |\Phi_2^{(2)}\rangle_{ij}, \tag{25}$$

where

$$|\Phi_1^{(1)}\rangle = (\cos\Gamma|0\rangle + e^{i\Delta}\sin\Gamma|1\rangle),$$

$$\begin{aligned}|\Phi_2^{(2)}\rangle = {} & (\cos\delta_1|00\rangle + e^{i\phi_2}\sin\delta_1\cos\delta_2|01\rangle \\ & + e^{i\phi_3}\sin\delta_1\sin\delta_2\cos\delta_3|10\rangle \\ & + e^{i\phi_4}\sin\delta_1\sin\delta_2\sin\delta_3|11\rangle),\end{aligned} \tag{26}$$

where, in Eqs. (26) we have dropped the subscripts $i,j,k=1,2,3$ $(i\neq j\neq k)$ denoting the three parties, because in the following we will deal with states invariant under permutation of any two qubits. In order to evaluate $E_G^{(2)}$ for the three-qubit $|W^{(3)}\rangle$ and $|\mathrm{GHZ}^{(3)}\rangle$ states we take advantage of the fact that the coefficients appearing in the definition of these states are all positive constants. Therefore, maximization of the overlaps with the states (26) does not depend on the phases, which can then be put to zero: $\Delta=\phi_q=0$ $(q=2,3,4)$. From Eq. (8), we get the following expression of the overlap for the state $|W^{(3)}\rangle$:

$$\begin{aligned}\Lambda_2^2(|W^{(3)}\rangle) = \max_{\{\delta_1,\delta_2,\delta_3,\Gamma\}} \frac{1}{3}[&\cos\delta_1\sin\Gamma + \cos\Gamma\sin\delta_1 \\ &\times(\cos\delta_2 + \sin\delta_2\cos\delta_3)]^2.\end{aligned} \tag{27}$$

The maximization in Eq. (27) yields the absolute maximum $\Lambda_2^2(|W^{(3)}\rangle)=2/3$. For instance, this value is reached when $\delta_1=\frac{\pi}{2}$, $\delta_2=\frac{\pi}{4}$, $\delta_3=0$, and $\Gamma=0$. It is then straightforward to verify that the tripartite component of the geometric entanglement present in the three-qubit W state is

$$E_G^{(2)}(|W^{(3)}\rangle) = \frac{1}{3}. \tag{28}$$

We see that for tripartite W states the purely tripartite contribution is strictly lower than the global geometric entanglement: $E_G^{(2)}(|W^{(3)}\rangle)=1/3<E_G^{(3)}(|W^{(3)}\rangle)=5/9$. On the other hand, for the state $|\mathrm{GHZ}^{(3)}\rangle$ the maximum overlap with the biseparable states is

$$\begin{aligned}\Lambda_2^2(|\mathrm{GHZ}^{(3)}\rangle) = \max_{\{\delta_1,\delta_2,\delta_3,\Gamma\}} \frac{1}{2}(&\cos\delta_1\cos\Gamma \\ &+ \sin\Gamma\sin\delta_1\sin\delta_2\sin\delta_3)^2.\end{aligned} \tag{29}$$

Direct computation yields

$$E_G^{(2)}(|\mathrm{GHZ}^{(3)}\rangle) = \frac{1}{2}. \tag{30}$$

Thus, in the case of GHZ states we verify that the tripartite and the global content of geometric entanglement coincide: $E_G^{(2)}(|\mathrm{GHZ}^{(3)}\rangle)=E_G^{(3)}(|\mathrm{GHZ}^{(3)}\rangle)=1/2$. This result is an independent proof that GHZ states possess only genuine tripartite entanglement. Moreover, we see that the tripartite entanglement of W states is less than that of GHZ states: $E_G^{(2)}(|W^{(3)}\rangle)<E_G^{(2)}(|\mathrm{GHZ}^{(3)}\rangle)$. This result clarifies the original finding by Wei and Goldbart that the global geometric entanglement $E_G^{(3)}(|W^{(3)}\rangle)$ of W states is larger than that, $E_G^{(3)}(|\mathrm{GHZ}^{(3)}\rangle)$, of GHZ states, and establishes a proper entanglement hierarchy between the two classes of states.

We now show how the structure of K separability allows us to clarify the nature of the geometric phases in the entanglement of superpositions. With this aim, let us calculate the distance $E_G^{(2)}$ for the superpositions (18) and (19); the corresponding behavior is reported in Fig. 2 as a function of η. Comparing with Fig. 1, we note that both $E_G^{(3)}$ and $E_G^{(2)}$ exhibit the same symmetric behavior for the superposition (18), and acquires a minimum at $\eta=\frac{\pi}{4}$. On the other hand, for the state (19) we observe that $E_G^{(2)}$, in contrast to $E_G^{(3)}$, is independent of the phase ϕ. This implies that the nonlocal nature of the phase ϕ is limited to the set S_2 of biseparable states.

B. Symmetric states: $\mathrm{GHZ}^{(N)}$ and $W^{(N)}$ states

In this section we study the properties of the measure (7) for the states $|\mathrm{GHZ}^{(N)}\rangle$ and $|W^{(N)}\rangle$ for arbitrary N. Concerning GHZ states, it is easily verified that, for any N,

$$E_G^{(K)}(|\mathrm{GHZ}^{(N)}\rangle) = \frac{1}{2}, \quad K = 2, \ldots, N. \tag{31}$$

Therefore, if we determine the various forms of bipartite and multipartite entanglement by the geometric measure (7), we obtain that the N-qubit GHZ states possess only N-partite entanglement.

Considering $|W^{(N)}\rangle$ states, for a given N all the bipartite and multipartite components of the geometric entanglement can be evaluated analytically with respect to the different K-separable states. First we study in detail the N-partite entanglement quantified by the distance $E_G^{(2)}(M_1|M_2)$ from the set of biseparable states $|\Phi\rangle = |\Phi_1^{(M_1)}\rangle \otimes |\Phi_2^{(M_2)}\rangle$, for a fixed bipartition M_1, $M_2 = N - M_1$, with $1 \leq M_1 \leq M_2 \leq N-1$. In this case, using Eq. (22), $|\Phi\rangle$ takes the form

$$|\Phi\rangle = \sum_{J_1=0}^{d_{M_1}-1} c_{J_1}^{(1)} |J_1\rangle\rangle_{M_1} \otimes \sum_{J_2=0}^{d_{M_2}-1} c_{J_2}^{(2)} |J_2\rangle\rangle_{M_2}, \tag{32}$$

with $c_{J_s}^{(s)} = r_{J_s}^{(s)} e^{i\phi_{J_s}^{(s)}}$, $s = 1, 2$, and, without loss of generality, we let $\phi_{J_s}^{(s)} = 0$, $s = 1, 2$. By exploiting the decomposition

$$\sum_{p=0}^{N-1} |2^p\rangle\rangle_N = \sum_{p=0}^{M_2-1} |0\rangle\rangle_{M_1} \otimes |2^p\rangle\rangle_{M_2} + \sum_{p=0}^{M_1-1} |2^p\rangle\rangle_{M_1} \otimes |0\rangle\rangle_{M_2}, \tag{33}$$

one has that the overlap $\Lambda_2^2(M_1|M_2)$ can be expressed in the form

$$\Lambda_2^2(M_1|M_2) = \max_{\{r_{J_s}^{(s)}\}} \frac{1}{N} \left(r_0^{(1)} \sum_{p=0}^{M_2-1} r_{2^p}^{(2)} + r_0^{(2)} \sum_{p=0}^{M_1-1} r_{2^p}^{(1)} \right)^2.$$

The maximization procedure is reported in Appendix B [see Eq. (B5)]. Using this result, in the case of two separability with respect to the partitioning $M \otimes (N-M)$, with $M \leq N - M$, the $K=2$ component of the geometric entanglement in the states $|W^{(N)}\rangle$ is

$$E_G^{(2)}(M|N-M) = \frac{M}{N}. \tag{34}$$

In the particular instance $M=1$, it immediately follows that the expression (34) realizes the absolute minimum Eq. (7), and therefore one has $E_G^{(2)}(|W^{(N)}\rangle) \equiv E_G^{(2)}(1|N-1) = 1/N$, showing that the genuine N-partite geometric entanglement vanishes asymptotically for large N. On the other hand, for the partition obtained by setting $M = [N/2]$, where $[x]$ denotes the integer part of x, the $K=2$ component of the geometric entanglement tends to the asymptotic limit 1/2 for large N. The limit coincides with the maximum possible value, attained by the $|\mathrm{GHZ}^{(N)}\rangle$ states.

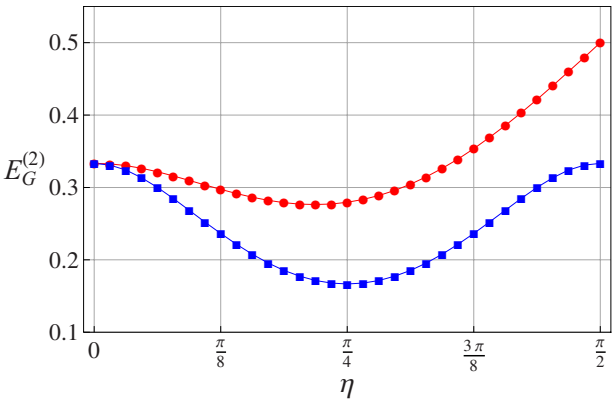

FIG. 2. (Color online) Behavior of $E_G^{(2)}$ for the superpositions of $|W^{(3)}\rangle$ and $|\tilde{W}^{(3)}\rangle$ (blue line with squares), Eq. (18), and for the superpositions of $|W^{(3)}\rangle$ and $|\mathrm{GHZ}^{(3)}\rangle$ (red lines with circles), Eq. (19), as a function of η, and for arbitrary phase ϕ. All plotted quantities are dimensionless.

We turn now to the determination of the generic K components of the (relative) multipartite geometric entanglement quantified, for arbitrary K, by the distance $E_G^{(K)}(M_1|\cdots|M_K)$ from the set of K-separable states for a given partition. We begin by rewriting the generic K-separable state in the form

$$|\Phi\rangle = \bigotimes_{s=1}^{K} \sum_{J_s=0}^{d_{M_s}-1} r_{J_s}^{(s)} |J_s\rangle\rangle_{M_s}, \tag{35}$$

where we recall that the ordering is $1 \leq M_1 \leq M_2 \leq \cdots \leq M_K \leq N-K+1$, with $\Sigma_{s=1}^K M_s = N$. In analogy with the previous analysis for the case $K=2$, it is not difficult to show that the squared overlap $\Lambda_K^2(M_1|\cdots|M_K)$ can be recast in the form

$$\Lambda_K^2(M_1|\cdots|M_K) = \max_{\{r_{J_s}^{(s)}\}} \frac{1}{N} \left(r_0^{(1)} r_0^{(2)} \cdots r_0^{(K-1)} \sum_{p=0}^{M_K-1} r_{2^p}^{(K)} + r_0^{(1)} r_0^{(2)} \cdots \sum_{p=0}^{M_{K-1}-1} r_{2^p}^{(K-1)} r_0^{(K)} + \cdots + \sum_{p=0}^{M_1-1} r_{2^p}^{(1)} r_0^{(2)} \cdots r_0^{(K-1)} r_0^{(K)} \right)^2. \tag{36}$$

By a partial maximization (see Appendix B), Eq. (B6) reduces to

$$\Lambda_K^2(M_1|\ldots|M_K) = \max_{\{\delta_0^{(s)}\}} \frac{1}{N}(\cos\delta_0^{(1)}\cos\delta_0^{(2)}\cdots\cos\delta_0^{(K-1)}\sin\delta_0^{(K)}\sqrt{M_K} + \cos\delta_0^{(1)}\cos\delta_0^{(2)}\cdots\cos\delta_0^{(K-2)}\sin\delta_0^{(K-1)}\cos\delta_0^{(K)}\sqrt{M_{K-1}} + \cdots + \sin\delta_0^{(1)}\cos\delta_0^{(2)}\cdots\cos\delta_0^{(K-1)}\cos\delta_0^{(K)}\sqrt{M_1})^2. \quad (37)$$

The explicit solution of the problem cannot be given for generic K: One needs to assign a specific value of K in order to solve the problem completely. In principle, full analytic solutions can always be obtained; however, the complexity of the problem grows with K, so that for sufficiently large values of K the help of numerical codes may become necessary. On the other hand, resorting to numerics, when necessary, poses no particular problem, as all the equations are rigorously defined and their recursive structures completely determined. Therefore, the complete analytic and numerical solutions can always be obtained on demand, for each arbitrarily assigned value of K and N, and according to the specific physical problem and type of multipartite state one is looking at.

Remarkably, from Eq. (37) it follows that the multipartite geometric entanglement of $|W^{(N)}\rangle$ states satisfies a property of self-similarity and scale invariance. Namely, given an N-qubit $|W^{(N)}\rangle$ state associated with a partition $M_1|\,M_2|\cdots|M_K$, let us take an integer L and consider the LN-qubit state $|W^{(LN)}\rangle$ associated with the scaled partition $LM_1|\,LM_2|\cdots|LM_K$. By Eq. (37), one immediately has that

$$\Lambda_K^2(M_1|\,M_2|\cdots|M_K) = \Lambda_K^2(LM_1|\,LM_2|\cdots|LM_K). \quad (38)$$

Thus, the K-partite geometric measures of entanglement enjoy the following property of scale invariance:

$$E_G^{(K)}(M_1|\,M_2|\cdots|M_K) = E_G^{(K)}(LM_1|\,LM_2|\cdots|LM_K). \quad (39)$$

Since relation (39) applies for *any* partition, it follows that it holds true for the absolute minimum, Eq. (7), as well. Finally, it is worth noticing that the property of scale invariance of the geometric measures of entanglement is trivially enjoyed by every GHZ state.

Proceeding with the discussion of the general case, we report the explicit analytic expression for the K component, with $K=3$, of the multipartite geometric entanglement of $|W^{(N)}\rangle$ states. The absolute minimum distance $E_G^{(3)}(|W^{(N)}\rangle)$ from the set of all three-separable states $\mathbf{S}_3$, which measures the N- and $(N-1)$-partite entanglement of $|W^{(N)}\rangle$ states, reads

$$E_G^{(3)}(|W^{(N)}\rangle) = \min\{E_{G>}^{(3)}(M_1|M_2|M_3), E_{G<}^{(3)}(M_1|M_2|M_3)\}, \quad (40)$$

where

$$E_{G>}^{(3)}(M_1|M_2|M_3) = 1 - \frac{M_3}{N}, \quad M_3 \geq M_1 + M_2, \quad (41)$$

$$E_{G<}^{(3)}(M_1|M_2|M_3) = 1 - \frac{4M_1M_2M_3}{N\Sigma}, \quad M_3 \leq M_1 + M_2, \quad (42)$$

with $\Sigma = 2(M_1M_2 + M_1M_3 + M_2M_3) - M_1^2 - M_2^2 - M_3^2$. The two expressions coincide when $M_3 = M_1 + M_2$.

In the following we present and discuss the solutions of Eq. (37). We will determine the associated $E_G^{(K)}(M_1|\,M_2|\cdots|M_K)$ for various choices of N and $M_1,\ldots,M_K$, and compare them with respect to a reference standard fixed by the $|\mathrm{GHZ}^{(N)}\rangle$ state. Finally, we will establish for each N the absolute minimum yielding $E_G^{(K)}(|W^{(N)}\rangle)$.

In Table I we report the exact values of the different geometric entanglements corresponding to all the possible K partitions in the case $N=4$. As already stated, in the $|\mathrm{GHZ}^{(4)}\rangle$ state the various components all coincide with the genuine four-partite entanglement. In the $|W^{(4)}\rangle$ state one has that for $K=3$ and 4, due to the symmetry under exchange of any pair of qubits, there is a unique way to partition the system, and the relative component of the geometric entanglement coincides with the absolute component. In the case $K=2$ one has two inequivalent possible partitions, and, as already proved in the general case, the absolute minimum is attained for the partition $1|3 \equiv 1|(N-1)$.

In Tables II and III we report the different multipartite components of the geometric entanglement, respectively in

TABLE I. Geometric measures of entanglement $E_G^{(K)}(M_1|\cdots|M_K)$, with $K=2,3,4$, for the four-qubit states $|\mathrm{GHZ}^{(4)}\rangle$ and $|W^{(4)}\rangle$.

	$\lvert\mathrm{GHZ}^{(4)}\rangle$	$\lvert W^{(4)}\rangle$
$E_G^{(4)}(1\vert\,1\vert 1\vert 1)$	1/2	37/64
$E_G^{(3)}(1\vert 1\vert 2)$	1/2	1/2
$E_G^{(2)}(\,2\vert 2)$	1/2	1/2
$E_G^{(2)}(\,1\vert 3)$	1/2	1/4

TABLE II. Geometric measures of entanglement $E_G^{(K)}(M_1|\cdots|M_K)$, with $K=2,3,4,5$, for the state $|W^{(5)}\rangle$.

	$\lvert W^{(5)}\rangle$		$\lvert W^{(5)}\rangle$
$E_G^{(5)}(1\vert 1\vert 1\vert 1\vert 1)$	0.590	$E_G^{(3)}(1\vert 1\vert 3)$	2/5
$E_G^{(4)}(1\vert\,1\vert 1\vert 2)$	0.559	$E_G^{(2)}(\,2\vert 3)$	2/5
$E_G^{(3)}(1\vert 2\vert 2)$	19/35	$E_G^{(2)}(\,1\vert 4)$	1/5

TABLE III. Geometric measures of entanglement $E_G^{(K)}(M_1|\cdots|M_K)$, with $K=2,3,4,5,6$, for the state $|W^{(6)}\rangle$.

	$\|W^{(6)}\rangle$		$\|W^{(6)}\rangle$
$E_G^{(6)}(1\|1\|\ 1\|1\|1\|1)$	0.598	$E_G^{(3)}(1\|2\|3)$	1/2
$E_G^{(5)}(1\|1\|1\|1\|2)$	0.580	$E_G^{(2)}(\ 3\|3)$	1/2
$E_G^{(4)}(1\|\ 1\|2\|2)$	0.567	$E_G^{(3)}(1\|1\|4)$	1/3
$E_G^{(3)}(2\|2\|2)$	5/9	$E_G^{(2)}(\ 2\|4)$	1/3
$E_G^{(4)}(1\|\ 1\|1\|3)$	1/2	$E_G^{(2)}(\ 1\|5)$	1/6

the $|W^{(5)}\rangle$ and $|W^{(6)}\rangle$ states. The fixed reference value 1/2 of the $|\mathrm{GHZ}\rangle$ states is not reported. From Tables II and III we see that for $N\geq 5$ there appear sets $S_K(M_1|\cdots|M_K)$ containing inequivalent partitions also for $K>2$. Moreover, we observe that the relative distances do not obey a definite hierarchy; for instance, from Table III we see that $E_G^{(3)}(2|2|2) > E_G^{(4)}(1|\ 1|1|3)$. However, and more importantly, the hierarchy of absolute distances is never violated. For instance, $\min E_G^{(3)}(M_1|M_2|M_3) < \min E_G^{(4)}(M_1|\ M_2|M_3|M_4)$, in perfect agreement with the general ordering established by Eq. (20).

Finally, we remark that all the measures evaluated analytically are rational numbers, and that the ones computed numerically appear to be approximations of rational numbers. Therefore, we conjecture that, for every *finite* N, all the relative and absolute multipartite geometric measures of entanglement are expressed by rational numbers.

C. Superpositions of $W^{(N)}$ and $|\mathrm{GHZ}^{(N)}\rangle$ states

It is of interest to investigate symmetric states constituted by generic superpositions of W and GHZ states:

$$|W\ \mathrm{GHZ}^{(N)}\rangle = \cos\ \eta|W^{(N)}\rangle + \sin\ \eta|\mathrm{GHZ}^{(N)}\rangle, \tag{43}$$

where the N-qubit $|\mathrm{GHZ}^{(N)}\rangle$ and $W^{(N)}$ states are defined by Eqs. (23) and (24), respectively. The squared overlap $\Lambda_2^2(\ M_1|M_2)$ associated with the set of biseparable states (32) can be computed exactly. One has

$$\Lambda_2^2(\ M_1|M_2) = \max_{\{r_{J_s}^{(s)}\}} \left[\frac{\cos\ \eta}{\sqrt{N}} \left(r_0^{(1)} \sum_{p=0}^{M_2-1} r_{2^p}^{(2)} + r_0^{(2)} \sum_{p=0}^{M_1-1} r_{2^p}^{(1)} \right) + \frac{\sin\ \eta}{\sqrt{2}} (r_0^{(1)} r_0^{(2)} + r_{2^{M_1}-1}^{(1)} r_{2^{M_2}-1}^{(2)}) \right]^2. \tag{44}$$

As shown in Appendix B, a partial maximization procedure reduces the above relation to

$$\begin{aligned}\Lambda_2^2(\ M_1|M_2) = \max_{\{\delta_q^{(s)}\}} \Bigg| & \frac{\cos\ \eta}{\sqrt{N}} (\cos\ \delta_0^{(1)} \sin\ \delta_0^{(2)} \sin\ \delta_1^{(2)} \sqrt{M_2} \\ & + \sin\ \delta_0^{(1)} \sin\ \delta_1^{(1)} \sin\ \delta_0^{(2)} \sqrt{M_1}) \\ & + \frac{\sin\ \eta}{\sqrt{2}} (\cos\ \delta_0^{(1)} \cos\ \delta_0^{(2)} \\ & + \sin\ \delta_0^{(1)} \cos\ \delta_1^{(1)} \sin\ \delta_0^{(2)} \cos\ \delta_1^{(2)}) \Bigg|^2. \end{aligned} \tag{45}$$

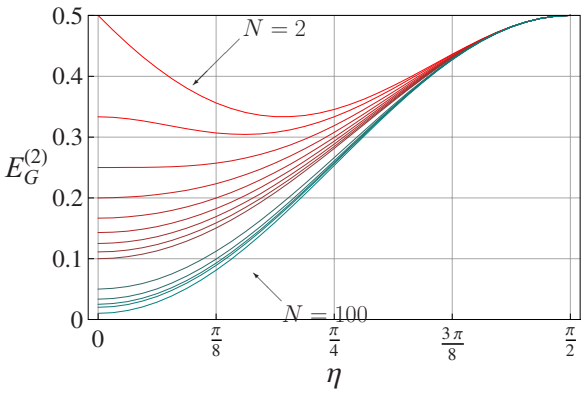

FIG. 3. (Color online) Behavior of $E_G^{(2)}(\ 1|N-1)$ in the superposition states Eq. (43), as a function of η, for $N=2,3,\ldots,10$, and for $N=20,30,40,50,100$. Curves are ordered from top to bottom with increasing N, with the uppermost curve corresponding to $N=2$ and the lowermost curve corresponding to $N=100$. All plotted quantities are dimensionless.

It is rather straightforward to prove that Eq. (45) and the associated geometric measure of entanglement enjoy the property of scale invariance $\Lambda_2^2(\ M_1|M_2)=\Lambda_2^2(\ LM_1|LM_2)$ (with L integer), where $\Lambda_2^2(\ LM_1|LM_2)$ is the squared overlap associated with the LN-qubit superposition state $|W\ \mathrm{GHZ}^{(LN)}\rangle$. At fixed values of η, M_1, and M_2, numerical evaluation of Eq. (45) can always be carried out easily. Being particularly interested in the quantification of genuine multipartite entanglement, we evaluate the geometric measure $E_G^{(2)}(\ 1|N-1)$, and report it in Fig. 3 for different values of N.

For $N=2$, the state $|W\ \mathrm{GHZ}^{(2)}\rangle$ reduces to a superposition of Bell states. In this case, $E_G^{(2)}(\ 1|1)$ attains the maximum value 1/2 at $\eta=0,\frac{\pi}{2}$. For $N=3$, the curve coincides with the one plotted in Fig. 2. Let us notice that in the instances $N=2,3$, absolute minima exist in the interval $(0,\frac{\pi}{2})$. For $N\geq 4$, $E_G^{(2)}(\ 1|N-1)$ increases monotonically from the value $1/N$ attained in the $|W^{(N)}\rangle$ state to the value 1/2 attained in the $|\mathrm{GHZ}^{(N)}\rangle$ state.

D. $N=4$ cluster state

In this section we apply the formalism previously introduced to the determination of the multipartite geometric entanglement of N-qubit cluster states [35] in the case $N=4$, the only nontrivial instance that allows an explicit closed expression. In fact, the $N=4$ cluster state can be expressed as a superposition of the form

$$|\mathrm{Cls}^{(4)}\rangle = \frac{1}{2}(|0000\rangle + |0011\rangle + |1100\rangle - |1111\rangle). \tag{46}$$

Recently, this state has been produced and characterized experimentally [36,37], as a relevant representative of the class of stabilizer states, which are very important both from a theoretical perspective and from a practical point of view for their property of entanglement persistency and for the implementation of one-way quantum computation [38].

In Table IV we report the values of the different components of the geometric entanglement in the $N=4$ cluster state

TABLE IV. Multipartite geometric measures of entanglement $E_G^{(K)}(M_1|\cdots|M_K)$, for $K=2,3,4$, in the four-qubit cluster state $|\mathrm{Cls}^{(4)}\rangle$.

	$E_G^{(4)}(1\|\,1\|1\|1)$	$E_G^{(3)}(1\|1\|2)$	$E_G^{(2)}(\,2\|2)$	$E_G^{(2)}(\,1\|3)$
$\|\mathrm{Cls}^{(4)}\rangle$	3/4	1/2	1/2	1/2

corresponding to all the possible K partitions of the four-partite system. We observe that in the case of $N=4$ cluster states there is a degeneracy in the geometric structure, as the absolute minimum is realized not only by the genuine four-partite components of entanglement $E_G^{(2)}(\,1|3)$ and $E_G^{(2)}(\,2|2)$, but also by the tripartite component $E_G^{(3)}(|\mathrm{Cls}^{(4)}\rangle)$. The latter coincides with $E_G^{(2)}(|\mathrm{Cls}^{(4)}\rangle)$. On the other hand, as $E_G^{(4)}(|\mathrm{Cls}^{(4)}\rangle) > E_G^{(3)}(|\mathrm{Cls}^{(4)}\rangle)$, the four-qubit cluster state possesses also a bipartite component besides the genuine four-partite contribution.

E. Magnon states

Going further toward higher generalizations that are physically significant, we discuss the class of symmetric N-qubit entangled states expressed as superpositions of magnon states [39,40]. A magnon is an elementary excitation of magnetic materials, i.e., a quantum of a spin wave, and W states are actually the simplest superpositions of all possible magnon states containing only one excitation. In the generic case of k excitations on N particles, the multimagnon superposition states can be written in the form

$$|\mathrm{Mg}_k^{(N)}\rangle = \binom{N}{k}^{-1/2} \sum_{p_k=k-1}^{N-1} \sum_{p_{k-1}=k-2}^{p_k-1} \times \cdots \times \sum_{p_1=0}^{p_2-1} |\, 2^{p_k} + 2^{p_{k-1}} + \cdots + 2^{p_1}\rangle\rangle_N, \quad (47)$$

For the sake of illustration, let us consider explicitly the case $k=2$, i.e., the superpositions of all possible N-qubit states containing two elementary excitations. Such states can be expressed in the form

$$|\mathrm{Mg}_2^{(N)}\rangle = \binom{N}{2}^{-1/2} \sum_{p=1}^{N-1} \sum_{q=0}^{p-1} |\, 2^p + 2^q\rangle\rangle_N, \quad (48)$$

with $N \geq 4$. In Table V we report the values, computed numerically, of the different components of the geometric entanglement in the four-qubit two-magnon state $|\mathrm{Mg}_2^{(4)}\rangle$.

By comparing Tables V, I, and IV, we see that, with respect to the $|W^{(4)}\rangle$ state, the $|\mathrm{Mg}_2^{(4)}\rangle$ state possesses enhanced genuine multipartite entanglement:

TABLE V. Geometric measures of entanglement $E_G^{(K)}(M_1|\cdots|M_K)$, with $K=2,3,4$, for the four-qubit magnon state $|\mathrm{Mg}_2^{(4)}\rangle$.

	$E_G^{(4)}(1\|\,1\|1\|1)$	$E_G^{(3)}(1\|1\|2)$	$E_G^{(2)}(\,2\|2)$	$E_G^{(2)}(\,1\|3)$
$\|\mathrm{Mg}_2^{(4)}\rangle$	0.625	0.583	1/3	1/2

$$E_G^{(2)}(|\mathrm{Mg}_2^{(4)}\rangle) = \min\{E_G^{(2)}(\,2|2); E_G^{(2)}(\,1|3)\}$$

$$= 1/3 > E_G^{(2)}(|W^{(4)}\rangle) = 1/4.$$

Analogously, the tripartite component $E_G^{(3)}(1|1|2)$ is enhanced in the magnon state compared to the W state. On the contrary, the $|\mathrm{Mg}_2^{(4)}\rangle$ state possesses a smaller amount of genuine multipartite entanglement compared to the $|\mathrm{Cls}^{(4)}\rangle$ state, while the tripartite component $E_G^{(3)}(1|1|2)$ is larger.

Next, we generalize the previous analysis to the case of N-qubit two-magnon states (48) with arbitrary N, and determine the geometric measure of entanglement $E_G^{(2)}(\,M_1|M_2)$, i.e., the distance from the set of two-separable states of the form (32). By exploiting the decomposition

$$\sum_{p=1}^{N-1} \sum_{q=0}^{p-1} |\, 2^p + 2^q\rangle\rangle_N = \sum_{p=1}^{M_2-1} \sum_{q=0}^{p-1} |\, 0\rangle\rangle_{M_1} \otimes |\, 2^p + 2^q\rangle\rangle_{M_2} + \sum_{p=1}^{M_1-1} \sum_{q=0}^{p-1} |\, 2^p + 2^q\rangle\rangle_{M_1} \otimes |\, 0\rangle\rangle_{M_2} + \sum_{p=0}^{M_1-1} |\, 2^p\rangle\rangle_{M_1} \otimes \sum_{p=0}^{M_2-1} |\, 2^p\rangle\rangle_{M_2}, \quad (49)$$

the squared overlap $\Lambda_2^2(\,M_1|M_2)$ can be written

$$\Lambda_2^2(\,M_1|M_2) = \binom{N}{2}^{-1} \max_{\{r_{J_s}^{(s)}\}} \left(r_0^{(1)} \sum_{p=1}^{M_2-1} \sum_{q=0}^{p-1} r_{2^p+2^q}^{(2)} + r_0^{(2)} \sum_{p=1}^{M_1-1} \sum_{q=0}^{p-1} r_{2^p+2^q}^{(1)} + \sum_{p=0}^{M_1-1} r_{2^p}^{(1)} \sum_{p=0}^{M_2-1} r_{2^p}^{(2)} \right)^2. \quad (50)$$

The mathematical details concerning the maximization of Eq. (50) are treated in Appendix C. From Eq. (C8), fixing $M=M_1 \leq M_2 = N-M$, we obtain

$$\Lambda_2^2(\,M|N-M) = [N(N-1)]^{-1} \max\{(N-M)(N-M-1); 2M(N-M)\}. \quad (51)$$

As in the previous instances of symmetric states, the squared overlap $\Lambda_2^2(\,M_1|N_2)$ and the corresponding geometric measure satisfy the property of scale invariance also for magnon states. One has: $\Lambda_2^2(\,M_1|N_2) = \Lambda_2^2(\,LM_1|LN_2)$ (with L integer), $\Lambda_2^2(\,LM_1|LN_2)$ being the squared overlap associated with the LN-qubit two-magnon state $|\mathrm{Mg}_2^{(LN)}\rangle$. For $M_1=1$ and $M_2=N-1$, the relation (51) reduces to $E_G^{(2)}(\,1|N-1)=2/N$, with $N \geq 4$. Therefore, the genuine N-partite geometric entanglement contained in two-magnon states vanishes asymptotically in the limit of large N, analogously to the case of N-qubit W states. This property is expected to hold in every multimagnon state: At any fixed, finite value of k, the genuine N-partite entanglement contained in a k-magnon state vanishes in the limit of large N.

IV. ASYMMETRIC STATES: GENERALIZED *W*-LIKE SUPERPOSITION STATES

In this section, we evaluate the geometric measure of entanglement for the class of asymmetric, generalized N-qubit W-like superposition states defined as

$$|\psi_W^{(N)}\rangle = \mathcal{N}_N \sum_{p=0}^{N-1} \gamma_{p+1} e^{i\xi_{p+1}} |\, 2^p\rangle\rangle_N, \tag{52}$$

where γ_p are real parameters, ξ_p are real phases, and the normalization factor is $\mathcal{N}_N = (\Sigma_{p=0}^{N-1} \gamma_{p+1}^2)^{-1/2}$. These states play a relevant role in quantum-information science according to the following considerations. It is well known that true tripartite entanglement of the state of a system of three qubits can be classified on the basis of stochastic local operations and classical communications. Such states can then be classified into two categories corresponding to the GHZ and W states. It is known that GHZ states can be used for teleportation and superdense coding, but the standard symmetric W states cannot. However, it has been shown that the class of asymmetric, generalized W-like superposition states (52) can be used as entangled resources for the implementation of perfect teleportation and superdense coding [41]. Moreover, several methods for their preparation have been proposed [42].

Without loss of generality and information content in the definition of the state, we assume $\gamma_p \in [0,1]$ and $\xi_p \in [0, 2\pi]$. Moreover, in the following, we will let $\xi_p = 0$ as it can be shown that the phases are irrelevant in the calculation of the geometric measures, being always canceled by the free phases of the K-separable states in the maximization procedure. The states (52) are asymmetric, i.e., not invariant with respect to the permutation of any pair of qubits. We first give explicit examples of application for the three-qubit and four-qubit instances, Eq. (52) with $N=3,4$ respectively. In the three-qubit case, proceeding as in Sec. III A, we compute the squared overlap (6) for the state $|\psi_W^{(3)}\rangle$. Dealing with asymmetric states, we have to specify the elementary qubits contained in the two sets Q_1 and Q_2 which determine the set $S_2(Q_1|Q_2)$ of the two-separable states. Thus, we compute the quantity $\Lambda_2^2(i|j,k)$, where $i,j,k=1,2,3$ with $i \neq j \neq k$ denote the three elementary qubits. The calculation of this quantity yields

$$\Lambda_2^2(i|j,k) = \mathcal{N}_3^2 \max\{\gamma_i^2, \gamma_j^2 + \gamma_k^2\}. \tag{53}$$

In Fig. 4, we plot the relative geometric measure $E_G^{(2)}(1|2,3)$ for the state $|\psi_W^{(3)}\rangle$ as a function of the variables γ_1 and γ_2, at a fixed value of γ_3. We see that $E_G^{(2)}(1|2,3)$ is formed by two surfaces whose curve of separation stays at the maximum attainable value 1/2. Similar plots can be obtained for $E_G^{(2)}(2|1,3)$ and $E_G^{(2)}(3|1,2)$. The absolute geometric measure of entanglement, as defined in Eq. (7), is given by $E_G^{(2)}(|\psi_W^{(3)}\rangle) = \min_{\{i,j,k\}}\{E_G^{(2)}(i|j,k)\}$ with $i,j,k=1,2,3$ and $i \neq j \neq k$; the absolute minimum is evaluated with respect to all possible permutations of the indices, as the state is not symmetric under the exchange of any two qubits. The absolute measure of geometric entanglement with respect to biseparable states is plotted in Fig. 5. The surface describing

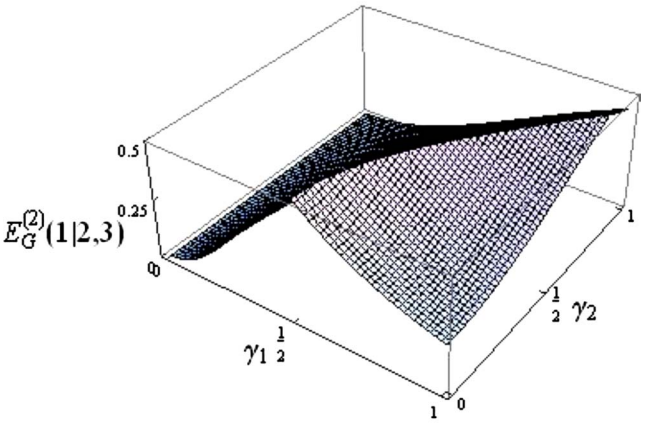

FIG. 4. (Color online) Relative measure of geometric entanglement $E_G^{(2)}(1|2,3)$ for the state $|\psi_W^{(3)}\rangle$, plotted as a function of γ_1 and γ_2, at fixed $\gamma_3 = 1/2$. All plotted quantities are dimensionless.

$E_G^{(2)}(|\psi_W^{(3)}\rangle)$ is formed by the contributions of three surfaces whose common intersection is at the absolute maximum 1/3. Let us notice that this absolute maximum is always achieved for $\gamma_1 = \gamma_2 = \gamma_3$.

In the case $N=4$, besides the bipartition $1|3$, we also have to take into account the bipartition $2|2$. Direct evaluation yields

$$\Lambda_2^2(i|j,k,l) = \mathcal{N}_4^2 \max\{\gamma_i^2, \gamma_j^2 + \gamma_k^2 + \gamma_l^2\}, \tag{54}$$

$$\Lambda_2^2(i,j|k,l) = \mathcal{N}_4^2 \max\{\gamma_i^2 + \gamma_j^2, \gamma_k^2 + \gamma_l^2\}. \tag{55}$$

The relative geometric measures $E_G^{(2)}(1|2,3,4)$ and $E_G^{(2)}(1,2|3,4)$ are plotted in Figs. 6 and 7, respectively, as functions of γ_1 and γ_2, at fixed γ_3 and γ_4. Similarly to the plot in Fig. 4, these three-dimensional plots are characterized by two surfaces whose separation curve is set at the maximum value 1/2. The absolute geometric measure $E_G^{(2)}(|\psi_W^{(4)}\rangle)$

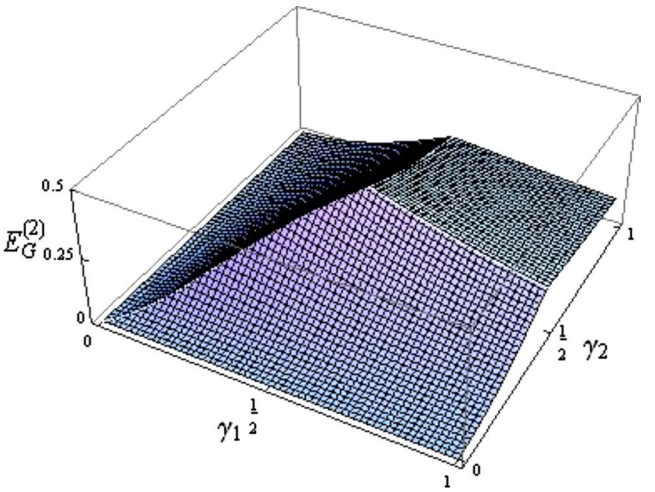

FIG. 5. (Color online) Absolute measure of geometric entanglement $E_G^{(2)}(|\psi_W^{(3)}\rangle)$, plotted as a function of γ_1 and γ_2, at fixed $\gamma_3 = 1/2$. All plotted quantities are dimensionless.

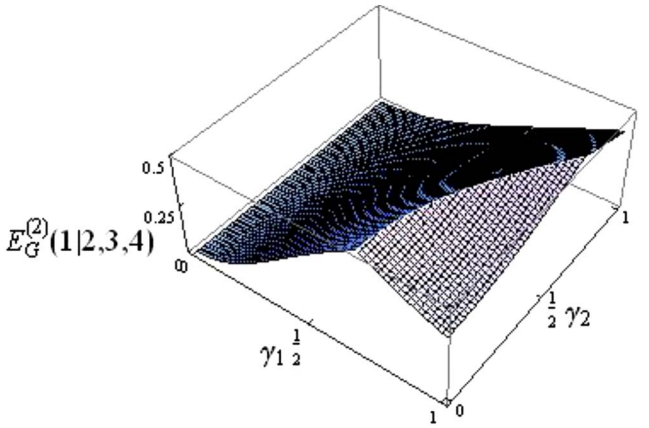

FIG. 6. (Color online) Relative measure of geometric entanglement $E_G^{(2)}(1|2,3,4)$ for the state $|\psi_W^{(4)}\rangle$, plotted as a function of γ_1 and γ_2, at fixed $\gamma_3=2/3$ and $\gamma_4=1/6$. All plotted quantities are dimensionless.

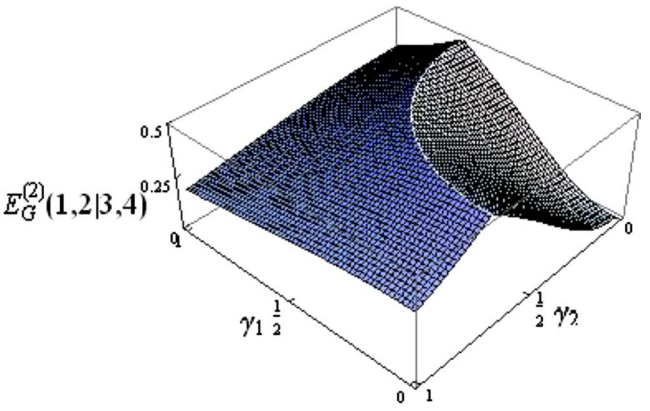

FIG. 7. (Color online) Relative measure of geometric entanglement $E_G^{(2)}(1,2|3,4)$ for the state $|\psi_W^{(4)}\rangle$, plotted as a function of γ_1 and γ_2, at fixed $\gamma_3=2/3$ and $\gamma_4=1/6$. All plotted quantities are dimensionless.

exhibits a behavior similar to that observed for the three-qubit instance; see Fig. 5.

We finally consider the general instance of N-qubit states, expressed by Eq. (52) for arbitrary N (with $\xi_{p+1}=0$). We compute the squared overlap $\Lambda_K^2(Q_1|\cdots|Q_K)$ associated with the K-separable state (3). For simplicity, we choose $Q_1=\{1,\ldots,M_1\}$, $Q_2=\{M_1+1,\ldots,M_1+M_2\}$, …, $Q_K=\{M_1+\cdots+M_{K-1}+1,\ldots,N\}$. Direct evaluation yields

$$\Lambda_K^2(Q_1|\cdots|Q_K)=\max_{\{r_{J_s}^{(s)}\}}\mathcal{N}_N^2\Bigg(r_0^{(1)}r_0^{(2)}\cdots r_0^{(K-1)}\sum_{p=0}^{M_K-1}r_{2^p}^{(K)}\gamma_{p+1}+r_0^{(1)}r_0^{(2)}\cdots\sum_{p=0}^{M_{K-1}-1}r_{2^p}^{(K-1)}\gamma_{p+1+M_K}r_0^{(K)}+\cdots+\sum_{p=0}^{M_1-1}r_{2^p}^{(1)}\gamma_{p+1+M_2+\cdots+M_K}r_0^{(2)}\cdots r_0^{(K)}\Bigg)^2. \tag{56}$$

The partial maximization of Eq. (56) (see Appendix B) yields the relation

$$\Lambda_K^2(Q_1|\cdots|Q_K)=\max_{\{\delta_0^{(s)}\}}\mathcal{N}_N^2(\cos\delta_0^{(1)}\cdots\cos\delta_0^{(K-1)}\sin\delta_0^{(K)}\sqrt{\sum_{p=0}^{M_K-1}\gamma_{p+1}^2}+\cos\delta_0^{(1)}\cdots\cos\delta_0^{(K-2)}\sin\delta_0^{(K-1)}\cos\delta_0^{(K)}\times\sqrt{\sum_{p=0}^{M_{K-1}-1}\gamma_{p+1+M_K}^2}+\cdots+\sin\delta_0^{(1)}\cos\delta_0^{(2)}\cdots\cos\delta_0^{(K)}\sqrt{\sum_{p=0}^{M_1-1}\gamma_{p+1+M_2+\cdots+M_K}^2})^2. \tag{57}$$

As with Eq. (37), in order to obtain the final result from the simplified relation (57), one needs to perform a (numerical) maximization only over K variables. It is straightforward to observe that Eq. (57) reduces to Eq. (37) for $\gamma_{p+1}=1$ for every p. Moreover, given Eq. (57), the results (53)–(55) are immediately recovered as particular cases.

V. CONCLUSIONS AND OUTLOOK

In this work we have introduced and discussed a class of generalized geometric measures of entanglement. For pure quantum states of N elementary subsystems, these extended measures are defined as the distances from the sets of K-separable states ($K=2,\ldots,N$). In principle, the entire set of these $N-1$ geometric measures provides a complete quantification and a hierarchical ordering of the different bipartite and multipartite components of the global geometric entanglement, and allows discrimination among the different multiparty contributions. After introducing and elucidating the fundamental properties of the generalized geometric measures, we have investigated in detail multipartite pure states of N-qubit systems. For the multiqubit case, we have derived some general properties of the extended geometric measures and discussed a systematic method for their evaluation in symmetric states including $W(N)$ states, GHZ(N) states, and their superpositions; symmetric cluster states; and

multimagnon states. Moreover, considering asymmetric states, we have introduced a method for the systematic determination of the multipartite components of geometric entanglement in a large class of generalized *W*-like superposition states. We have identified a property of self-similarity and scale invariance holding for all types of geometric entanglement and symmetric multipartite pure states of many-qubit systems. Finally, in a series of mathematical appendixes, we have sketched the main mathematical framework needed for the exact numerical and/or analytical evaluation of the bipartite and multipartite components of geometric entanglement in any, arbitrarily chosen, pure state of many-qubit systems.

A challenge of great potential interest is to extend the mathematical framework and the recursive computation schemes developed for multiqubit states to higher-dimensional quantum systems. A further significant issue concerns the extension of the geometric setting to mixed states, beyond the immediate, but in practice not very useful, procedures based on the convex hull construction. Devising alternative, but conceptually equally satisfactory, extensions would be especially important in order to establish a deeper understanding of the possible operational characterizations for the set of geometric measures of entanglement in the presence of classical noise and non unitary quantum operations. Finally, it would be important to investigate to what extent the multicomponent measures of geometric entanglement defined in the present work could be exploited to construct geometric monotones obeying a structure of shared entanglement and monogamy bounds for distributed entanglement, and their role in the understanding of quantum critical phenomena and quantum cooperative systems.

ACKNOWLEDGMENTS

We acknowledge MIUR under PRIN National Project 2005, CNR-INFM Research and Development Center "Coherentia," INFN, and the ISI Foundation for financial support.

APPENDIX A: HYPERSPHERICAL PARAMETRIZATION

A very convenient parametrization for the moduli r_J in Eq. (22), that automatically solves the normalization constraint, is the representation in hyperspherical coordinates in d_M dimensions:

$$\begin{aligned} v_0 &= \cos\,\delta_0, \\ v_1 &= \sin\,\delta_0 \cos\,\delta_1, \\ &\vdots \\ v_{d_M-2} &= \sin\,\delta_0 \cdots \sin\,\delta_{d_M-3} \cos\,\delta_{d_M-2}, \\ v_{d_M-1} &= \sin\,\delta_0 \cdots \sin\,\delta_{d_M-3} \sin\,\delta_{d_M-2}, \end{aligned} \tag{A1}$$

where δ_L are angles with values in the interval $[0,\frac{\pi}{2}]$. Let us note that the one-to-one mapping between r_J and v_L (with $J,L=0,\ldots,d_M-1$), or equivalently between the indices J and L, can be chosen by following a suitable ordering. In fact, the term v_L will be constituted by a product of L trigonometric functions; thus, it would be convenient to have expressions involving parameters v_L with low values of the index L. Considering the state (22), the most immediate choice for r_J is obtained by letting $r_J=v_J$ for $J=0,\ldots,d_M-1$. Interpreting the two levels 0 and 1 of the single qubit as the ground and the excited levels, respectively, of the elementary system, a further useful choice for the mapping between J and L can be obtained by associating the parameter v_L with the coefficient r_J of the N-qubit ket in the order of growing number of excitations. Let us recall that, for an arbitrary N-qubit state, the global ground state $|00\ldots0\rangle$ is labeled by the index $J=0$; the kets with single excitation, e.g., of the form $|010\ldots0\rangle$, are labeled by the indices $J=2^p$ with $p=0,\ldots,N-1$; the kets with two excitations, e.g., of the form $|01010\ldots0\rangle$, are labeled by the indices $J=2^q+2^s$ with $q=1,\ldots,N-1$ and $s=0,\ldots,p-1$; and so on. One can decide to choose the following mapping for the parametrization:

$$\begin{aligned} r_0 &= v_0, \\ r_{2^p} &= v_{p+1}, \quad p=0,\ldots,N-1, \\ r_{2^q+2^s} &= v_{N+q+s}, \\ q &= 1,\ldots,N-1, s=0,\ldots,q-1, \\ &\vdots . \end{aligned} \tag{A2}$$

Clearly, the choice of the mapping between r_J and v_L can be suitably made by looking at the terms that survive in the squared overlap (6).

APPENDIX B: EVALUATION OF EQS. (33), (36), (44), and (56)

Here we outline the analytical evaluation of the squared overlaps (33), (36), (44), and (56). The quantity $\Lambda_2^2(M_1|M_2)$ in Eq. (33) involves only coefficients of the form $r_0^{(s)}$ and $r_{2^p}^{(s)}$ $(s=1,2)$. Therefore, when using the hyperspherical representation (A1), by exploiting the freedom in the ordering, we choose the mapping given in Eq. (A2), specifically

$$\begin{aligned} r_0^{(s)} &= v_0^{(s)} = \cos\,\delta_0, \\ r_{2^p}^{(s)} &= v_{p+1}^{(s)} = \sin\,\delta_0^{(s)} \cdots \sin\,\delta_p^{(s)} \cos\,\delta_{p+1}^{(s)}, \\ p &= 0,\ldots,M_s-1. \end{aligned} \tag{B1}$$

Such parametrization leads to the explicit expression

$$\begin{aligned} \Lambda_2^2(M_1|M_2) = \max_{\{\delta_{J_s}^{(s)}\}} \frac{1}{N} [&\cos\,\delta_0^{(1)} \sin\,\delta_0^{(2)} (\cos\,\delta_1^{(2)} \\ &+ \sin\,\delta_1^{(2)} \{\cos\,\delta_2^{(2)} + \sin\,\delta_2^{(2)} [\cdots (\cos\,\delta_{M_2-1}^{(2)} \\ &+ \sin\,\delta_{M_2-1}^{(2)} \cos\,\delta_{M_2}^{(2)})]\}) \end{aligned}$$

$$+\cos\ \delta_0^{(2)}\ \sin\ \delta_0^{(1)}\cos\ \delta_1^{(1)}$$
$$+\sin\ \delta_1^{(1)}\{\cos\ \delta_2^{(1)}+\sin\ \delta_2^{(1)}[\cdots(\cos\ \delta_{M_1-1}^{(1)}$$
$$+\sin\ \delta_{M_1-1}^{(1)})\cos\ \delta_{M_1}^{(1)}]\}]^2. \quad \text{(B2)}$$

Analyzing the structure of the $|W^{(N)}\rangle$ states, it is convenient, given a generic integer M, and a set of generic variables δ_i, $i=1,\ldots,M$, to introduce the following function:

$$f(\delta_1^{(s)},\ldots,\delta_{M_s}^{(s)})=\cos\ \delta_1^{(s)}+\sin\ \delta_1^{(s)}\{\cos\ \delta_2^{(s)}+\sin\ \delta_2^{(s)}$$
$$\times[\cdots(\cos\ \delta_{M_s-1}^{(s)}+\sin\ \delta_{M_s-1}^{(s)}\cos\ \delta_{M_s}^{(s)})]\}. \quad \text{(B3)}$$

By means of Eq. (B3), the expression (B2) can be recast in the more compact form

$$\Lambda_2^2(M_1|M_2)=\max_{\{\delta_{J_s}^{(s)}\}}\frac{1}{N}\{\cos\ \delta_0^{(1)}\ \sin\ \delta_0^{(2)}f(\delta_1^{(2)},\ldots,\delta_{M_2}^{(2)})$$
$$+\cos\ \delta_0^{(2)}\ \sin\ \delta_0^{(1)}f(\delta_1^{(1)},\ldots,\delta_{M_1}^{(1)})\}^2. \quad \text{(B4)}$$

To proceed, we first maximize the function $f(\delta_1^{(s)},\ldots,\delta_M^{(s)})$, i.e., Eq. (B3), over the M_s independent variables $\delta_h^{(s)}$ $(h=1,\ldots,M_s)$. This task can be accomplished as follows: First, trivially, $\delta_M^{(s)}=0$ maximizes $\cos\ \delta_M^{(s)}$. Next, the contribution $(\cos\ \delta_{M-1}^{(s)}+\sin\ \delta_{M-1}^{(s)})$ reaches the maximum value $\sqrt{2}$ for $\delta_{M-1}^{(s)}=\frac{\pi}{4}$. After the elimination of the parameters $\delta_{M-1}^{(s)}$ and $\delta_M^{(s)}$, the term $(\cos\ \delta_{M-2}^{(s)}+\sin\ \delta_{M-2}^{(s)}\sqrt{2})$ appears. Observing that terms of the form $(\cos\ \theta+\sin\ \theta\sqrt{n})$ acquire the maximum value $\sqrt{1+n}$ for $\theta=\arcsin\sqrt{\frac{n}{1+n}}$, the cascade maximization procedure yields that Eq. (B3) is maximized at the value $\sqrt{M_s}$ for $\delta_{M-h}^{(s)}=\arcsin\sqrt{\frac{h}{1+h}}$, with $h=0,1,\ldots,M-1$. Recalling that $1\leq M_1\leq M_2=N-M_1$ and performing the final maximization in Eq. (B2) yields

$$\Lambda_2^2(M_1|M_2)=\frac{M_2}{N}. \quad \text{(B5)}$$

The above maximum overlap squared is reached for the values $\delta_0^{(1)}=0$, $\delta_0^{(2)}=\frac{\pi}{2}$, and $\delta_{N-M-h}^{(2)}=\arcsin\sqrt{\frac{h}{h+1}}$ with $h=0,1,\ldots,M_2-1$.

One can now consider the squared overlap $\Lambda_K^2(M_1|\cdots|M_K)$, Eq. (36). Proceeding as for Eq. (33), and thus using, for any s, the hyperspherical representation (A1) with the mapping given by Eq. (B1), one can express Eq. (36) in terms of the angular parameters $\delta_{J_s}^{(s)}$. Moreover, by using definition (B3),

$$\Lambda_K^2(M_1|\cdots|M_K)=\max_{\{\delta_{J_s}^{(s)}\}}\frac{1}{N}[\cos\ \delta_0^{(1)}\ \cos\ \delta_0^{(2)}\cdots\cos\ \delta_0^{(K-1)}\sin\ \delta_0^{(K)}f(\delta_1^{(K)},\ldots,\delta_{M_K}^{(K)})+\cos\ \delta_0^{(1)}\ \cos\ \delta_0^{(2)}\cdots\cos\ \delta_0^{(K-2)}$$
$$\times\sin\ \delta_0^{(K-1)}f(\delta_1^{(K-1)},\ldots,\delta_{M_{K-1}}^{(K-1)})\cos\ \delta_0^{(K)}+\cdots+\sin\ \delta_0^{(1)}f(\delta_1^{(1)},\ldots,\delta_{M_1}^{(1)})\times\ \times\cos\ \delta_0^{(2)}\cdots\cos\ \delta_0^{(K-1)}\ \cos\ \delta_0^{(K)}]^2. \quad \text{(B6)}$$

The maximization of the functions f, corresponding to the replacement $f(\delta_1^{(s)},\ldots,\delta_{M_s}^{(s)})\rightarrow\sqrt{M_s}$, reduces relation (B6) to Eq. (37).

Next, we consider the squared overlap (44). By choosing the mapping

$$r_0^{(s)}=v_0^{(s)}=\cos\ \delta_0^{(s)},$$
$$r_{2M_s-1}^{(s)}=v_1^{(s)}=\sin\ \delta_0^{(s)}\cos\ \delta_1^{(s)},$$
$$r_{2^p}^{(s)}=v_{p+2}^{(s)}=\sin\ \delta_0^{(s)}\cdots\sin\ \delta_{p+1}^{(s)}\cos\ \delta_{p+2}^{(s)},$$
$$p=0,\ldots,M_s-1, \quad \text{(B7)}$$

we obtain the relation

$$\Lambda_2^2(M_1|M_2)=\max_{\{\delta_q^{(s)}\}}\left|\frac{\cos\ \eta}{\sqrt{N}}[\cos\ \delta_0^{(1)}\ \sin\ \delta_0^{(2)}\ \sin\ \delta_1^{(2)}\right.$$
$$\times f(\delta_2^{(2)},\ldots,\delta_{M_2+1}^{(2)})$$
$$+\sin\ \delta_0^{(1)}\ \sin\ \delta_1^{(1)}\ \sin\ \delta_0^{(2)}f(\delta_2^{(1)},\ldots,\delta_{M_1+1}^{(1)})]$$
$$+\frac{\sin\ \eta}{\sqrt{2}}(\cos\ \delta_0^{(1)}\ \cos\ \delta_0^{(2)}$$
$$\left.+\sin\ \delta_0^{(1)}\cos\ \delta_1^{(1)}\ \sin\ \delta_0^{(2)}\ \cos\ \delta_1^{(2)})\right|^2. \quad \text{(B8)}$$

By maximizing the functions f, we arrive at the final expression Eq. (45).

Coming to the squared overlap $\Lambda_K^2(Q_1|\cdots|Q_K)$, i.e., Eq. (56), one can proceed as for Eq. (36) in order to obtain a relation identical to Eq. (B6) with the functions f replaced by the functions F defined as

$$F(\delta_1^{(s)},\ldots,\delta_{M_s}^{(s)}) = \Gamma_1^{(s)}\cos\delta_1^{(s)} + \sin\delta_1^{(s)}\{\Gamma_2^{(s)}\cos\delta_2^{(s)} + \sin\delta_2^{(s)} \times[\cdots(\Gamma_{M_s-1}^{(s)}\cos\delta_{M_s-1}^{(s)} + \sin\delta_{M_s-1}^{(s)} \times\Gamma_{M_s}^{(s)}\cos\delta_{M_s}^{(s)})]\}, \tag{B9}$$

where $\Gamma_{p+1}^{(s)} = \gamma_{p+1+M_{s+1}+\cdots+M_K}$, with $p=0,\ldots,M_s-1$. It is straightforward to notice that the following relation holds:

$$\max_{\delta}\{x\cos\delta + y\sin\delta\} = \sqrt{x^2+y^2}, \tag{B10}$$

where x and y are real parameters. By exploiting iteratively the maximization procedure for terms of this form, we find that Eq. (B9) is maximized at the value $\sqrt{\Sigma_{p=0}^{M_s-1}(\Gamma_{p+1}^{(s)})^2}$. Finally, by maximizing all the functions F, the squared overlap (56) reduces to Eq. (57).

APPENDIX C: EVALUATION OF EQ. (50)

In order to compute the squared overlap $\Lambda_2^2(M_1|M_2)$, Eq. (50), we exploit again the hyperspherical coordinates (A1), and we introduce the following mapping:

$$r_0^{(s)} = v_0^{(s)} = \cos\delta_0^{(s)},$$

$$r_{2^p+2^q}^{(s)} = v_{l(p,q)+1}^{(s)} = \sin\delta_0^{(s)}\cdots\sin\delta_{l(p,q)}^{(s)}\cos\delta_{l(p,q)+1}^{(s)},$$

$$l(p,q) = 0,\ldots,L_s-1, \quad p=1,\ldots,M_s-1,$$

$$q = 0,\ldots,p-1,$$

$$r_{2^p}^{(s)} = v_{p+1+L_s}^{(s)} = \sin\delta_0^{(s)}\cdots\sin\delta_{p+L_s}^{(s)}\cos\delta_{p+1+L_s}^{(s)},$$

$$p = 0,\ldots,M_s-1, \tag{C1}$$

where . Furthermore, by defining the function

$$g(\delta_1^{(s)},\ldots,\delta_{L_s}^{(s)}) = \sin\delta_0^{(s)}\cdots\sin\delta_{L_s}^{(s)}, \tag{C2}$$

Eq. (50) is recast in the form

$$\Lambda_2^2(M_1|M_2) = \max_{\delta_{J_s}^{(s)}}|\sin\delta_0^{(1)}\cos\delta_0^{(2)} f(\delta_1^{(1)},\ldots,\delta_{L_1}^{(1)}) + \cos\delta_0^{(1)}\sin\delta_0^{(2)} f(\delta_1^{(2)},\ldots,\delta_{L_2}^{(2)}) + \sin\delta_0^{(1)}\sin\delta_0^{(2)} g(\delta_1^{(1)},\ldots,\delta_{L_1}^{(1)}) \times f(\delta_{1+L_1}^{(1)},\ldots,\delta_{M_1+L_1}^{(1)}) g(\delta_1^{(2)},\ldots,\delta_{L_2}^{(2)}) \times f(\delta_{1+L_2}^{(2)},\ldots,\delta_{M_2+L_2}^{(2)})|^2. \tag{C3}$$

The functions $f(\delta_{1+L_s}^{(s)},\ldots,\delta_{M_s+L_s}^{(s)})$ in the last term of Eq. (C3) can be maximized at the value $\sqrt{M_s}$. It is quite straightforward to observe that the functions f and g are connected by the relation

$$f(\delta_1^{(s)},\ldots,\delta_{L_s}^{(s)}) = f(\delta_1^{(s)},\ldots,\delta_{L_s-1}^{(s)}) + g(\delta_1^{(s)},\ldots,\delta_{L_s-1}^{(s)})\cos\delta_{L_s}. \tag{C4}$$

By using property (C4) and applying the maximization relation (B10) to the variables $\delta_{L_1}^{(1)},\delta_{L_1-1}^{(1)},\ldots,\delta_1^{(1)},\delta_0^{(1)}$, Eq. (C3) reduces to

$$\Lambda_2^2(M_1|M_2) = \max_{\delta_{J_2}^{(2)}}\binom{N}{2}^{-1}\{\cos^2\delta_0^{(2)}L_1 + \sin^2\delta_0^{(2)} \times[f^2(\delta_1^{(2)},\ldots,\delta_{L_2}^{(2)}) + g^2(\delta_1^{(2)},\ldots,\delta_{L_2}^{(2)})M_1M_2]\}. \tag{C5}$$

Observing that $L_1 < L_2, M_1M_2$, a further maximization on the variable $\delta_0^{(2)}$ yields

$$\Lambda_2^2(M_1|M_2) = \max_{\delta_{J_2}^{(2)}}\binom{N}{2}^{-1}[f^2(\delta_1^{(2)},\ldots,\delta_{L_2}^{(2)}) + g^2(\delta_1^{(2)},\ldots,\delta_{L_2}^{(2)})M_1M_2]. \tag{C6}$$

In order to maximize Eq. (C6), one has to find the conditions for the vanishing of the first partial derivatives with respect to each variable $\delta_q^{(2)}$ with $q=1,\ldots,L_2$, and to select the absolute maximum in the intervals $0\le\delta_q^{(2)}\le\frac{\pi}{2}$. Without reporting the whole set of calculations, we outline briefly the main steps of the maximization procedure. The first partial derivative with respect to $\delta_{L_2}^{(2)}$ yields the following condition:

$$g(\delta_1^{(2)},\ldots,\delta_{L_2}^{(2)})[f(\delta_1^{(2)},\ldots,\delta_{L_2}^{(2)}) - M_1M_2 g(\delta_1^{(2)},\ldots,\delta_{L_2-1}^{(2)})\cos\delta_{L_2}^{(2)}] = 0. \tag{C7}$$

By using Eq. (C7) together with all the other partial derivatives with respect to $\delta_q^{(2)}$ $(q=1,\ldots,L_2-1)$, it is not difficult to verify that the absolute maximum of $\Lambda_2^2(M_1|M_2)$ is given by

$$\Lambda_2^2(M_1|M_2) = \binom{N}{2}^{-1}\max\{L_2, M_1M_2\}. \tag{C8}$$

Indeed, from Eq. (C7) one has that if $g(\delta_1^{(2)},\ldots,\delta_{L_2}^{(2)})=0$, then Eq. (C6) reduces to the maximization of the function $f(\delta_1^{(2)},\ldots,\delta_{L_2}^{(2)})$, i.e., $\sqrt{L_2}$. On the other hand, if

$$f(\delta_1^{(2)},\ldots,\delta_{L_2}^{(2)}) = M_1M_2 g(\delta_1^{(2)},\ldots,\delta_{L_2-1}^{(2)})\cos\delta_{L_2},$$

then the maximum is reached for $\delta_q=\frac{\pi}{2}$, i.e., $f(\frac{\pi}{2},\ldots,\frac{\pi}{2})=0$ and $g(\frac{\pi}{2},\ldots,\frac{\pi}{2})=1$. It can be verified that all the other values of δ_q leading to the vanishing of the first partial derivatives are associated with relative maxima.

[1] A. Einstein, B. Podolsky, and N. Rosen, Phys. Rev. **47**, 777 (1935).
[2] E. Schrödinger, Naturwiss. **23**, 807 (1935); **23**, 823 (1935); **23**, 844 (1935).
[3] C. H. Bennett, H. J. Bernstein, S. Popescu, and B. Schumacher, Phys. Rev. A **53**, 2046 (1996).
[4] C. H. Bennett, D. P. DiVincenzo, J. A. Smolin, and W. K. Wootters, Phys. Rev. A **54**, 3824 (1996).
[5] G. Vidal, J. Mod. Opt. **47**, 355 (2000).
[6] For recent comprehensive reviews on various aspects of entanglement theory, see M. Plenio and S. Virmani, Quantum Inf. Comput. **7**, 1 (2007); I. Bengtsson and K. Zyczkowski, *Geometry of Quantum States* (Cambridge University Press, Cambridge, U.K., 2006); R. Horodecki, P. Horodecki, M. Horodecki, and K. Horodecki, e-print arXiv:quant-ph/0702225.
[7] S. Popescu and D. Rohrlich, Phys. Rev. A **56**, R3319 (1997).
[8] V. Vedral and M. B. Plenio, Phys. Rev. A **57**, 1619 (1998).
[9] G. Vidal and R. F. Werner, Phys. Rev. A **65**, 032314 (2002).
[10] S. Hill and W. K. Wootters, Phys. Rev. Lett. **78**, 5022 (1997).
[11] W. K. Wootters, Phys. Rev. Lett. **80**, 2245 (1998).
[12] C. H. Bennett, S. Popescu, D. Rohrlich, J. A. Smolin, and A. V. Thapliyal, Phys. Rev. A **63**, 012307 (2000).
[13] W. Dür, G. Vidal, and J. I. Cirac, Phys. Rev. A **62**, 062314 (2000).
[14] F. Verstraete, J. Dehaene, B. De Moor, and H. Verschelde, Phys. Rev. A **65**, 052112 (2002).
[15] D. M. Greenberger, M. Horne, and A. Zeilinger, in *Bell's Theorem, Quantum Theory, and Conceptions of the Universe*, edited by M. Kafatos (Kluwer, Dordrecht, 1989).
[16] V. Coffman, J. Kundu, and W. K. Wootters, Phys. Rev. A **61**, 052306 (2000).
[17] J. Eisert and H. J. Briegel, Phys. Rev. A **64**, 022306 (2001).
[18] D. A. Meyer and N. R. Wallach, J. Math. Phys. **43**, 4273 (2002).
[19] G. K. Brennen, Quantum Inf. Comput. **3**, 619 (2003).
[20] A. J. Scott, Phys. Rev. A **69**, 052330 (2004).
[21] T. R. de Oliveira, G. Rigolin, and M. C. de Oliveira, Phys. Rev. A **73**, 010305(R) (2006); G. Rigolin, T. R. de Oliveira, and M. C. de Oliveira, *ibid.* **74**, 022314 (2006).
[22] P. Facchi, G. Florio, and S. Pascazio, Phys. Rev. A **74**, 042331 (2006).
[23] M. B. Plenio and V. Vedral, J. Phys. A **34**, 6997 (2001).
[24] A. Shimony, Ann. N. Y. Acad. Sci. **755**, 675 (1995).
[25] H. Barnum and N. Linden, J. Phys. A **34**, 6787 (2001).
[26] T.-C. Wei and P. M. Goldbart, Phys. Rev. A **68**, 042307 (2003).
[27] J. Eisert and D. Gross, in *Lectures on Quantum Information*, edited by D. Bruss and G. Leuchs (Wiley-VCH, Weinheim, 2006).
[28] D. Cavalcanti, Phys. Rev. A **73**, 044302 (2006).
[29] O. Gühne, M. Reimpell, and R. F. Werner, Phys. Rev. Lett. **98**, 110502 (2007).
[30] J. Eisert, F. G. S. L. Brandão, and K. M. R. Audenaert, New J. Phys. **9**, 46 (2007).
[31] T.-C. Wei, J. B. Altepeter, P. M. Goldbart, and W. J. Munro, Phys. Rev. A **70**, 022322 (2004).
[32] T.-C. Wei, D. Das, S. Mukhopadyay, S. Vishveshwara, and P. M. Goldbart, Phys. Rev. A **71**, 060305(R) (2005).
[33] R. Orús, Phys. Rev. Lett. **100**, 130502 (2008).
[34] R. Orús, S. Dusuel, and J. Vidal, e-print arXiv:0803.3151v1.
[35] H. J. Briegel and R. Raussendorf, Phys. Rev. Lett. **86**, 910 (2001).
[36] N. Kiesel, C. Schmid, U. Weber, G. Tóth, O. Gühne, R. Ursin, and H. Weinfurter, Phys. Rev. Lett. **95**, 210502 (2005).
[37] F. Dell'Anno, S. De Siena, and F. Illuminati, Phys. Rep. **428**, 53 (2006).
[38] R. Raussendorf and H. J. Briegel, Phys. Rev. Lett. **86**, 5188 (2001).
[39] D. C. Mattis, *The Theory of Magnetism I—Statics and Dynamics* (Springer-Verlag, Berlin, 1988).
[40] T. Morimae, A. Sugita, and A. Shimizu, Phys. Rev. A **71**, 032317 (2005).
[41] P. Agrawal and A. K. Pati, Phys. Rev. A **74**, 062320 (2006); S. Adhikari and S. Gangopadhyay, e-print arXiv:0803.0607.
[42] G. C. Guo and Y.-S. Zhang, Phys. Rev. A **65**, 054302 (2002); V. N. Gorbachev, A. A. Rodichkina, A. I. Trubilko, and A. I. Zhiliba, Phys. Lett. A **310**, 339 (2003); A. Biswas and G. S. Agarwal, J. Mod. Opt. **51**, 1627 (2004).